A *hp*-adaptive discontinuous Galerkin method for plasmonic waveguides

Stefano Giani[1]

School of Engineering and Computing Sciences Durham University , South Road, Durham, DH1 3LE United Kingdom

Abstract

In this paper we propose and analyse a *hp*-adaptive discontinuous finite element method for computing electromagnetic modes of propagation supported by waveguide structures comprised of a thin lossy metal film of finite width embedded in an infinite homogeneous dielectric. We propose a goal-oriented or dual weighted residual error estimator based on the solution of a dual problem that we use to drive the adaptive refinement with the aim to compute accurate approximation of the modes. We illustrate in the last section the benefits of the resulting *hp*-adaptive method in practice, which consist in fast convergence and accurate estimation of the error. We tested the method computing the vanishing modes for a metallic waveguide of square section.

Keywords:
discontinuous Galerkin methods, *a posteriori* error estimation, adaptivity, eigenvalue problems.
2000 MSC: 65N15, 65N30, 65N50, 35P99

1. Introduction

With the fast development of microfabrication technology, nanophotonics has received very high interest. As an important branch of nanophotonics, plasmonics has enabled light-matter interactions at a deep subwavelength length scale. Plasmonics, or surface plasmon based photonics, focus on how to exploit the optical property of metals. In this work probably the most simple plasmonic device, consisting in a metallic waveguide embedded in an infinite homogeneous dielectric, is analysed and used to assess the performances of the *hp*-adaptive method presented in this paper.

The goal-oriented error estimator derived in Section 4 is the adaptation to the plasmonic waveguides problem of the error estimator presented in [1].

The model problem considered in this work is defined on a rectangular domain Ω that is the union of two disjoint subdomains Ω_{out}, Ω_{in}, where Ω_{in} coincides with the section of the metallic waveguide and $\Omega_{\text{out}} := \Omega \setminus \Omega_{\text{in}}$. For simplicity we are going to consider only rectangular waveguides.

We also define three scalar functions $\mathcal{A}$, $\mathcal{B}$ and $\mathcal{C}$ that can assume a positive and real value in Ω_{out} and either a positive and real value also in Ω_{in} or a complex value in Ω_{in}. We are going to denote the values of $\mathcal{A}$, $\mathcal{B}$ and $\mathcal{C}$ in each subdomain with $\mathcal{A}_{\text{in}}$, $\mathcal{A}_{\text{out}}$, $\mathcal{B}_{\text{in}}$, $\mathcal{B}_{\text{out}}$, $\mathcal{C}_{\text{in}}$ and $\mathcal{C}_{\text{out}}$.

The model problem can be written in the following form: *seek eigenpairs of the form* $(\lambda, u) \in \mathbb{C} \times H_0^1(\Omega)$ *such that*

$$\int_\Omega (\nabla v)^* \mathcal{A} \nabla u - \mathcal{B} u \overline{v} \;=\; \lambda \int_\Omega \mathcal{C} u \overline{v} \quad \text{for all } v \in H_0^1(\Omega), \tag{1}$$

where * denotes Hermitian transpose and where we imposed Dirichlet homogeneous boundary conditions along the border of the domain as the domain has been truncated as explained in Section 2. In this work we assume that the interface $\Omega_{\text{in}} \cap \Omega_{\text{out}}$ is aligned with the meshes.

The outline of the paper is as follows. In Section 2 we briefly describe how problem (1) is derived from Maxwells equations. In Section 3 we introduce the discrete version of problem (1) and the discontinuous Galerkin method. In the following Section 4 the error estimator is presented and in Section 5 the adaptive algorithm is described. Finally in Section 6 we present some numerical results.

2. Plasmonics eigenvalue problems

The mathematical development (see e.g. [2]) begins with Maxwell's equations in frequency domain for a lossy inhomogeneous isotropic medium of a metallic waveguide of infinite length aligned with the z-axes and surrounded by dielectric material. Then uncoupling Maxwell's equations yields the following time-harmonic vectorial wave equations for the electric and magnetic fields:

$$\begin{aligned} &\nabla \times \nabla \times \mathbf{E} - \omega^2 \varepsilon \mu \mathbf{E} = 0 \ , \\ &\nabla \times \varepsilon^{-1} \nabla \times \mathbf{H} - \omega^2 \mu \mathbf{H} = 0 \ , \end{aligned} \tag{2}$$

where ω is the frequency, $\mathbf{E}$ is the electric field, $\mathbf{H}$ is the magnetic field, ε and μ are, respectively, the dielectric permittivity and magnetic permeability

tensors. Because of the assumptions, the dielectric permittivity ε is a scalar function in x and y only. Furthermore we assume that μ is homogeneous and for simplicity we assume that $\mu = 1$.

Due to the structure under consideration, that is invariant in the z direction, the mode fields vary along this dimension according to $e^{-\gamma z}$ where $\gamma = \alpha + i\beta$ is the complex propagation constant of the mode with α the attenuation constant and β the phase constant.

Then substituting this field form into (2) and considering the two polarization cases TE ($\mathbf{E}_x = 0$) and TH ($\mathbf{H}_x = 0$) we obtain a couple of uncoupled scalar equations:

$$\Delta \mathbf{E}_y + (\gamma^2 + \omega^2 \mu\varepsilon)\mathbf{E}_y = 0 \quad \text{(TE case)} , \tag{3}$$

$$\nabla \cdot (\varepsilon^{-1} \nabla \mathbf{H}_y) + (\gamma^2 \varepsilon^{-1} + \omega^2 \mu)\mathbf{H}_y = 0 \quad \text{(TM case)} . \tag{4}$$

Each of problems (3), (4) can be solved in two ways, either fixing γ and considering ω^2 as the eigenvalue or fixing ω and considering γ^2 as the eigenvalue. Anyway all of these problems may be written in the abstract form as that of seeking (λ, u) with $u \neq 0$ such that

$$\nabla \cdot (\mathcal{A} \nabla u) + \mathcal{B} u + \lambda \mathcal{C} u \ = \ 0 . \tag{5}$$

Since $\mathcal{A}$, $\mathcal{B}$ or $\mathcal{C}$ may be discontinuous, (5) has to be understood in an appropriate weak form. So far (5) is posed over all of $\mathbb{R}^2$. Problem (5) is difficult to solve numerically because it is posed on an unbounded domain. In order to make the problem more treatable, it is necessary to truncate the domain far enough away from the metallic guide. The resulting domain Ω is of rectangular shape with homogeneous Dirichlet boundary conditions. An analysis of the effect of truncation of the domain on self-adjoint problems with potential is done in [3]. In view of that and of the numerical results presented in [4] where the same approach was tested on photonic crystals, it seems that the truncation is stable for the modes confined on the surface of the metallic guide which decays exponentially away from the guide.

3. Discrete eigenvalue problems

In recent years discontinuous Galerkin (DG) methods for elliptic problems [5] have become increasingly popular. Some of the main reasons for this increase of interest in DG methods is that allowing for discontinuities

across elements gives extraordinary flexibility in terms of mesh design and choice of shape functions. Additionally, *hp*-DG, which are based on locally refined meshes and variable approximation orders, have been shown to achieve tremendous gains in computational efficiency for challenging problems [6, 7, 8, 9, 10, 1, 11, 12, 13].

Since we are going to construct sequences of adaptively refined shape-regular meshes, we denote the meshes by $\mathcal{T}_n$, where n is the index of the mesh. The meshes $\mathcal{T}_n$ are partitions of $\Omega \subset \mathbb{R}^2$ into open quadrilaterals $\{K\}_{K\in\mathcal{T}_n}$. We also assume that, in the interior of each element $K \in \mathcal{T}_n$, $\mathcal{A}$, $\mathcal{B}$ and $\mathcal{C}$ are smooth. In presence of jumping coefficients, the jumps are aligned with the meshes used in this work. The diameter of an element $K \in \mathcal{T}_n$ is denoted by h_K. Furthermore, we assume that these diameters are of bounded variation, that is, there is a constant $b_1 \geq 1$ such that

$$b_1^{-1} \leq h_K/h_{K'} \leq b_1, \tag{6}$$

whenever K and K' share a common edge. We store the diameters of the elements of $\mathcal{T}_n$ in the mesh size vector $\mathbf{h} = \{h_K \,:\, K \in \mathcal{T}_n\}$. Similarly, we associate with each element $K \in \mathcal{T}_n$ a polynomial degree $p_K \geq 1$ and define the degree vector $\mathbf{p} = \{p_K \,:\, K \in \mathcal{T}_n\}$. We assume that $\mathbf{p}$ is of bounded variation as well, that is, there is a constant $b_2 \geq 1$ such that

$$b_2^{-1} \leq p_K/p_{K'} \leq b_2, \tag{7}$$

whenever K and K' share a common edge.

For a partition $\mathcal{T}_n$ of Ω and a degree vector $\mathbf{p}$, we define the *hp*-version discontinuous Galerkin finite element space S_n of complex valued functions by

$$S_n = \{\, v \in L^2(\Omega) \,:\, v|_K \in \mathcal{P}_{p_K}(K),\ K \in \mathcal{T}_n \,\}, \tag{8}$$

where, $\mathcal{P}_{p_K}(K)$ is the space of polynomials on K of degree less or equal p_K in each dimension.

Next, we define some trace operators that are required for the DG methods. To this end, we denote by $\mathcal{E}_{\mathcal{I}}(\mathcal{T}_n)$ the set of all interior edges of the partition $\mathcal{T}_n$ of Ω, and by $\mathcal{E}_{\Gamma}(\mathcal{T}_n)$ the set of all boundary edges of $\mathcal{T}_n$. Furthermore, we define $\mathcal{E}(\mathcal{T}_n) = \mathcal{E}_{\mathcal{I}}(\mathcal{T}_n) \cup \mathcal{E}_{\Gamma}(\mathcal{T}_n)$. The boundary ∂K of an element K and the sets $\partial K \setminus \Gamma$ and $\partial K \cap \Gamma$ will be identified in a natural way with the corresponding subsets of $\mathcal{E}(\mathcal{T}_n)$.

Let K^+ and K^- be two adjacent elements of $\mathcal{T}_n$, and $e \in \mathcal{E}_{\mathcal{I}}(\mathcal{T}_n)$ given by $e = \partial K^+ \cap \partial K^-$. Furthermore, let v be a scalar-valued function, that is

smooth inside each element $K^{\pm}$. By $v^{\pm}$, we denote the traces of v on e taken from within the interior of $K^{\pm}$, respectively. Then, since we are dealing with jumping coefficients we need to use the definition of the weighted average of the diffusive flux $\mathcal{A}\nabla_n v$ along $e \in \mathcal{E}_{\mathcal{I}}(\mathcal{T}_n)$ introduced in [6]

$$\{\!\{\mathcal{A}\nabla_n v\}\!\}_w = \omega^-(\mathcal{A}\nabla_n v)^- + \omega^+(\mathcal{A}\nabla_n v)^+ \ ,$$

where

$$\omega^- = \frac{\mathbf{n}_{K^+}^t \mathcal{A}^+ \mathbf{n}_{K^+}}{\mathbf{n}_{K^-}^t \mathcal{A}^- \mathbf{n}_{K^-} + \mathbf{n}_{K^+}^t \mathcal{A}^+ \mathbf{n}_{K^+}} \ , \quad \omega^+ = \frac{\mathbf{n}_{K^-}^t \mathcal{A}^- \mathbf{n}_{K^-}}{\mathbf{n}_{K^-}^t \mathcal{A}^- \mathbf{n}_{K^-} + \mathbf{n}_{K^+}^t \mathcal{A}^+ \mathbf{n}_{K^+}} \ ,$$

where we denote by $\mathbf{n}_{K^\pm}$ the unit outward normal vector of $\partial K^{\pm}$, respectively. Similarly, for a scalar function we have the following weighted average

$$\{\!\{v\}\!\}_w = \omega^- v^+ + \omega^+ v^- \ .$$

Then, the jump of v across $e \in \mathcal{E}_{\mathcal{I}}(\mathcal{T}_n)$ is given by

$$[\![v]\!] = v^+ \, \mathbf{n}_{K^+} + v^- \, \mathbf{n}_{K^-},$$

$$[\![\mathcal{A}\nabla_n v]\!] = \mathcal{A}^+\nabla_n v^+ \cdot \mathbf{n}_{K^+} + \mathcal{A}^-\nabla_n v^- \cdot \mathbf{n}_{K^-}.$$

On a boundary edge $e \in \mathcal{E}_{\Gamma}(\mathcal{T}_n)$, we set $\{\!\{\mathcal{A}\nabla_n v\}\!\}_w = \mathcal{A}\nabla_n v$ and $[\![v]\!] = v\mathbf{n}$, with $\mathbf{n}$ denoting the unit outward normal vector on the boundary Γ.

Remark 3.1. *The weighted mean value $\{\!\{\cdot\}\!\}_w$ satisfies the following relation:*

$$(\mathcal{A}\nabla_n u)^+ \cdot \mathbf{n}_{K^+} v^+ + (\mathcal{A}\nabla_n u)^- \cdot \mathbf{n}_{K^-} v^- \ = \ \{\!\{\mathcal{A}\nabla_n u\}\!\}_w \cdot [\![v]\!] + [\![\mathcal{A}\nabla_n u]\!] \{\!\{v\}\!\}_w \ , \quad (9)$$

which is already a well-known result for the standard DG mean value.

For a mesh $\mathcal{T}_n$ on Ω and a polynomial degree vector $\mathbf{p}$, let S_n be the finite element space defined in (8). We consider the (symmetric) weighted interior penalty discretization [6] of (5): find $(\lambda_n, u_n) \in \mathbb{C} \times S_n$ such that

$$A_n(u_n, v) \ = \ \lambda_n b(u_n, v) \ , \quad \text{for all } v \in S_n \ , \qquad (10)$$

with $b(u_n, u_n) = 1$ and where

$$\begin{aligned} A_n(u,v) := & \sum_{K \in \mathcal{T}_n} \int_K \mathcal{A}_K \nabla_n u \cdot \nabla_n \overline{v} - \mathcal{B}_K u \overline{v} \, dx \\ & - \sum_{e \in \mathcal{E}(\mathcal{T}_n)} \int_e \left(\{\!\{\mathcal{A}\nabla_n \overline{v}\}\!\}_w \cdot [\![u]\!] + \{\!\{\mathcal{A}\nabla_n u\}\!\}_w \cdot [\![\overline{v}]\!] \right) ds + \sum_{e \in \mathcal{E}(\mathcal{T}_n)} \int_e \mathsf{c} \, [\![u]\!] \cdot [\![\overline{v}]\!] \, ds, \\ b(u,v) := & \int_\Omega u \, \mathcal{C} \, \overline{v} \, dx \ . \end{aligned}$$

Here, ∇_n denotes the element-wise gradient operator and $\mathcal{A}_K$ and $\mathcal{B}_K$ denote the restrictions of $\mathcal{A}$ and $\mathcal{B}$ onto K. Furthermore, the function $\mathtt{c} \in L^\infty(\mathcal{E}(\mathcal{T}_n))$ is the discontinuity stabilisation function that is chosen as follows: we define the functions $\mathtt{h} \in L^\infty(\mathcal{E}(\mathcal{T}_n))$ and $\mathtt{p} \in L^\infty(\mathcal{E}(\mathcal{T}_n))$ by

$$\mathtt{h}(\mathbf{r}) := \begin{cases} \min(h_{K^+}, h_{K^-}), & \mathbf{r} \in e \in \mathcal{E}_{\mathcal{I}}(\mathcal{T}_n),\ e = \partial K^+ \cap \partial K^-, \\ h_K, & \mathbf{r} \in e \in \mathcal{E}_{\Gamma}(\mathcal{T}_n),\ e \in \partial K \cap \Gamma, \end{cases}$$

$$\mathtt{p}(\mathbf{r}) := \begin{cases} \max(p_{K^+}, p_{K^-}), & \mathbf{r} \in e \in \mathcal{E}_{\mathcal{I}}(\mathcal{T}_n),\ e = \partial K^+ \cap \partial K^-, \\ p_K, & \mathbf{r} \in e \in \mathcal{E}_{\Gamma}(\mathcal{T}_n),\ e \in \partial K \cap \Gamma, \end{cases}$$

and set the penalty parameter to be

$$\mathtt{c} = \delta \gamma_K \frac{\mathtt{p}^2}{\mathtt{h}}, \tag{11}$$

with $\gamma_K = \omega^+ \mathbf{n}_{K^+}^t \mathcal{A}^+ \mathbf{n}_{K^+} = \omega^- \mathbf{n}_{K^-}^t \mathcal{A}^- \mathbf{n}_{K^-}$, and with a parameter $\delta > 0$ that is independent of $\mathbf{h}$, $\mathbf{p}$, $\mathcal{A}^+$ and $\mathcal{A}^-$. The parameter $\mathtt{c}$ defined here is an *hp*-version of the weighted penalty parameter [6].

4. Goal-oriented a posteriori error estimation

In this section we introduce the a posteriori analysis, which is based on an auxiliary problem described below. The analysis presented here follows the analysis already presented in [1] which was applied to different kinds of eigenvalue problems. The actual form of the auxiliary problem depends on the goal functional $J(\cdot)$ utilized. We note that, even if the primal problem (5) is non-linear, the auxiliary problem, which is related to the dual/adjoint operator in (5), is linear for our choice of $J(\cdot)$. It is interesting to remark that the analysis can be easily used with a different goal functional to obtain an automatic adaptive method to target particular measurements of the error. In this section we consider only a functional to estimate the error for eigenvalues.

From [14] we have that the minimum regularity for eigenfunctions of (5) on a domain with discontinuous coefficients of the kind we consider in the work is $u \in H^{1+2/3}(\Omega) \cap H_0^1(\Omega)$. Also from the theory in [14] we know that the eigenfunctions are continuous everywhere and that $\mathcal{A}\nabla u$ is continuous where $\mathcal{A}$ is smooth and it is continuous across the interfaces between different values of $\mathcal{A}$. Since we have assumed that the initial mesh, which resolves the

jumps of $\mathcal{A}$, is always conforming then it is not possible with our refinement procedure to have a face in any adapted mesh tangential to a corner of the interface between different values of $\mathcal{A}$. It a fortiori follows that across all faces of the mesh $\mathcal{A}\nabla u$ is continuous.

In order to proceed we recast the discrete problem (10) in a more suitable, but equivalent form: *seek eigenpairs* $\hat{u}_n := (\lambda_n, u_n) \in \mathbb{C} \times S_n$, *such that*

$$\mathcal{N}(\hat{u}_n, \hat{v}_n) \;=\; 0 \quad \forall \hat{v}_n = (\delta_n, v_n) \in \mathbb{C} \times S_n \;,$$

where

$$\mathcal{N}(\hat{u}_n, \hat{v}_n) := -A_n(u_n, v_n) + \lambda_n b(u_n, v_n) + \delta_n(\|u_n\|^2_{0,\mathcal{C}} - 1) \;, \tag{12}$$

where $\|\cdot\|_{0,\mathcal{C}}$ is the standard $L^2(\Omega)$ norm weighted by the coefficient $\mathcal{C}$.

Now, we briefly outline the key steps involved in estimating the error in the goal functional $J(\hat{u}) - J(\hat{u}_n)$ employing the Dual Weighted Residual (DWR) technique [15, 16], for a general target functional of practical interest $J(\cdot)$. Because the analysis is the same for many different definition of the functional $J(\cdot)$, we introduce its definition used in the numerical experiments only later in this section. For the moment we work with a general $J(\cdot)$ which is assumed to be differentiable. So, we write $\bar{J}(\cdot,\cdot;\cdot)$ to denote the mean value linearisation of $J(\cdot)$, defined by

$$\bar{J}(\hat{u}, \hat{u}_n; \hat{u} - \hat{u}_n) = J(\hat{u}) - J(\hat{u}_n) = \int_0^1 J'[\theta\hat{u} + (1-\theta)\hat{u}_n](\hat{u} - \hat{u}_n)\, d\theta \;,$$

where $J'[\hat{w}](\cdot)$ denotes the Fréchet derivative of $J(\cdot)$ evaluated at some $\hat{w} \in \mathbb{C} \times S$, and $S := S_n + \left(H^{1+2/3}(\Omega) \cap H^1_0(\Omega)\right)$ is the space of functions that are sum of a finite element function in S_n and a function in $H^{1+2/3}(\Omega) \cap H^1_0(\Omega)$. In the same way, we write

$$\mathcal{M}(\hat{u}, \hat{u}_n; \hat{u}-\hat{u}_n, \hat{w}) = \mathcal{N}(\hat{u}, \hat{w}) - \mathcal{N}(\hat{u}_n, \hat{w}) = \int_0^1 \mathcal{N}'_{\hat{u}}[\theta\hat{u}+(1-\theta)\hat{u}_n](\hat{u}-\hat{u}_n, \hat{w})\, d\theta \;.$$

We now introduce the following formal dual problem: find $\hat{z} \in \mathbb{C} \times S$ such that

$$\mathcal{M}(\hat{u}, \hat{u}_n; \hat{w}, \hat{z}) = \bar{J}(\hat{u}, \hat{u}_n; \hat{w}) \;, \quad \forall \hat{w} \in \mathbb{C} \times S \;. \tag{13}$$

We assume that (13) possesses a unique solution. This assumption is, of course, dependent on both the definition of $\mathcal{M}(\hat{u}, \hat{u}_n; \cdot, \cdot)$ and the target functional under consideration. For the proceeding error analysis, we must therefore assume that (13) is well-posed. In order to compute our error estimator

we are not going to solve (13), but compute a discrete approximation of it in order to obtain an accurate approximation of the dual solution $\hat{z}$.

The next theorem introduces the residual forming the error estimator and its corollary introduces a simple way to compute an upper bound of the error.

Lemma 4.1. *Let $\hat{u} \in \mathbb{C} \times \left(H^{1+2/3}(\Omega) \cap H_0^1(\Omega)\right)$ be an eigenpair of (5) with $\|u\|_{0,\mathcal{C}} = 1$, then for any $\hat{z} \in \mathbb{C} \times S$ we have*

$$\mathcal{N}(\hat{u}, \hat{z}) = 0 \ .$$

Proof. Without loss of generality we assume that $\hat{z} := (\delta, z_n + z_c)$, with $\delta \in \mathbb{C}$, $z_n \in S_n$ and $z_c \in H^{1+2/3}(\Omega) \cap H_0^1(\Omega)$. Applying (12) we have

$$\mathcal{N}(\hat{u}, \hat{z}) = -A_n(u, z_n+z_c)+\lambda b(u, z_n+z_c) = -A_n(u, z_n)+\lambda b(u, z_n)-A_n(u, z_c)+\lambda b(u, z_c) \ . \tag{14}$$

Because u is continuous and $\mathcal{A}\nabla_n u$ is continuous across the faces of the mesh we have by integration-by-parts and by using (9) that

$$\begin{aligned} A_n(u, z_n) \ &= \sum_{K \in \mathcal{T}_n} \int_K \mathcal{A}_K \nabla_n u \cdot \nabla_n \overline{z_n} - \mathcal{B}\, u\, \overline{z_n}\, dx - \sum_{e \in \mathcal{E}(\mathcal{T}_n)} \int_e \{\!\{\mathcal{A}\nabla_n u\}\!\}_w \cdot [\![\overline{z_n}]\!]\, ds \\ &= \int_\Omega -\nabla \cdot (\mathcal{A}\nabla u)\, \overline{z_n} - \mathcal{B}\, u\, \overline{z_n}\, dx = \lambda b(u, z_n) \ , \end{aligned} \tag{15}$$

it is useful to remark that the last integral is well-defined in the distribution sense because the test function z_n and $\mathcal{A}$ are smooth in the interior of each element. Similarly because z_c is continuous and its regularity is at least $H^{1+2/3}$, we have by integration-by-parts:

$$A_n(u, z_c) \ = \sum_{K \in \mathcal{T}_n} \int_K \mathcal{A}_K \nabla_n u \cdot \nabla_n \overline{z_c} - \mathcal{B}\, u\, \overline{z_c}\, dx = \lambda b(u, z_c) \ . \tag{16}$$

Substituting (15) and (16) into (14) we have the result. □

Theorem 4.2. *Let us denote by $\hat{z}_n$ the finite element approximation of $\hat{z}$ in S_n. Then*

$$J(\hat{u}) - J(\hat{u}_n) = -\mathcal{N}(\hat{u}_n, \hat{z} - \hat{z}_n) = \sum_{K \in \mathcal{T}_n} \eta_K \ , \quad \forall \hat{z}_n \in \mathbb{C} \times S_n \ ,$$

where the residual η_K is defined as:

$$\begin{aligned}\eta_K &= \int_K -(\lambda_n \mathcal{C}\ u_n + \nabla\cdot(\mathcal{A}_K\nabla u_n) + \mathcal{B}u_n)\overline{(z-z_n)}\,dx \\ &-\frac{1}{2}\int_{\partial K/\Gamma}\{\!\{\mathcal{A}\nabla\overline{(z-z_n)}\}\!\}_w\cdot[\![u_n]\!]\,ds + \frac{1}{2}\int_{\partial K/\Gamma}[\![\mathcal{A}\nabla u_n]\!]\{\!\{\overline{z-z_n}\}\!\}_w\,ds \\ &+\frac{1}{2}\int_{\partial K/\Gamma}\mathsf{c}[\![u_n]\!][\![\overline{z-z_n}]\!]\,ds - \int_{\partial K\cap\Gamma}\mathbf{n}\cdot(\mathcal{A}\nabla_n\overline{(z-z_n)})u_n\,ds + \int_{\partial K\cap\Gamma}\mathsf{c}u_n\overline{(z-z_n)}\,ds\ .\end{aligned}$$

Proof. From the formal dual problem (13) and by Lemma 4.1 we have that:

$$\begin{aligned}J(\hat{u})-J(\hat{u}_n) &= \bar{J}(\hat{u},\hat{u}_n;\hat{u}-\hat{u}_n) = \mathcal{M}(\hat{u},\hat{u}_n;\hat{u}-\hat{u}_n,\hat{z}) \\ &= \mathcal{N}(\hat{u},\hat{z})-\mathcal{N}(\hat{u}_n,\hat{z}) = -\mathcal{N}(\hat{u}_n,\hat{z}-\hat{z}_n)\ ,\end{aligned}$$

where in the last equality we used the fact that $\mathcal{N}(\hat{u}_n,\hat{z}_n)=0$. Then by the definition of $A_n(\cdot,\cdot)$ and since $\|u_n\|_{0,\mathcal{C}}=1$ we have:

$$\begin{aligned}-\mathcal{N}(\hat{u}_n,\hat{z}-\hat{z}_n) &= A_n(\hat{u}_n,z-z_n)-\lambda_n b(u_n,z-z_n) \\ &= \sum_{K\in\mathcal{T}_n}\int_K \mathcal{A}_K\nabla_n u_n\cdot\nabla_n\overline{(z-z_n)} - (\mathcal{B}u_n-\lambda_n\mathcal{C}u_n)\overline{(z-z_n)}\,dx \\ &\quad -\sum_{e\in\mathcal{E}(\mathcal{T}_n)}\int_e\left(\{\!\{\mathcal{A}\nabla_n\overline{(z-z_n)}\}\!\}_w\cdot[\![u_n]\!]+\{\!\{\mathcal{A}\nabla_n u_n\}\!\}_w\cdot[\![\overline{z-z_n}]\!]\right)ds \\ &\quad +\sum_{e\in\mathcal{E}(\mathcal{T}_n)}\int_e \mathsf{c}\,[\![u_n]\!]\cdot[\![\overline{z-z_n}]\!]\,ds\ .\end{aligned}$$

Integrating by parts the second-order term element-wise we obtain:

$$\begin{aligned}\sum_{K\in\mathcal{T}_n}\int_K \mathcal{A}_K\nabla_n u_n\cdot\nabla_n\overline{(z-z_n)}\,dx &= \sum_{K\in\mathcal{T}_n}\Big\{\int_K -\nabla_n\cdot(\mathcal{A}_K\nabla_n u_n)\overline{(z-z_n)}\,dx \\ &\quad +\int_{\partial K}\mathbf{n}_{K^+}\cdot(\mathcal{A}\nabla_n u_n)\overline{(z-z_n)}\,ds\Big\}.\end{aligned}$$

Using (9), the second term on the right hand side can then further be expanded to

$$\sum_{K\in\mathcal{T}_n}\int_{\partial K}\mathcal{A}_K\frac{\partial u_n}{\partial \mathbf{n}_{K^+}}\overline{(z-z_n)}\,ds=\sum_{e\in\mathcal{E}_{\mathcal{I}}(\mathcal{T}_n)}\int_e\{\!\{\mathcal{A}\nabla u_n\}\!\}_w\cdot[\![\overline{z-z_n}]\!]+[\![\mathcal{A}\nabla u_n]\!]\cdot\{\!\{\overline{z-z_n}\}\!\}_w\,ds$$
$$+\sum_{e\in\mathcal{E}_{\Gamma}(\mathcal{T}_n)}\int_e\mathbf{n}\cdot(\mathcal{A}\nabla_n u_n)\overline{(z-z_n)}\,ds\ .$$

Then substituting this back we finally obtain:

$$\begin{aligned}-\mathcal{N}(\hat{u}_n,\hat{z}-\hat{z}_n)\ &=\sum_{K\in\mathcal{T}_n}\int_K\big(-\nabla\cdot(\mathcal{A}_K\nabla u_n)-\mathcal{B}u_n-\lambda_n\mathcal{C}u_n\big)\overline{(z-z_n)}\,dx\\
&-\sum_{e\in\mathcal{E}_{\mathcal{I}}(\mathcal{T}_n)}\int_e\{\!\{\mathcal{A}\nabla_n\overline{(z-z_n)}\}\!\}_w\cdot[\![u_n]\!]\,ds+\sum_{e\in\mathcal{E}_{\mathcal{I}}(\mathcal{T}_n)}\int_e[\![\mathcal{A}\nabla u_n]\!]\{\!\{\overline{z-z_n}\}\!\}_w\,ds\\
&+\sum_{e\in\mathcal{E}_{\mathcal{I}}(\mathcal{T}_n)}\int_e\mathsf{c}\,[\![u_n]\!]\cdot[\![\overline{z-z_n}]\!]\,ds-\sum_{e\in\mathcal{E}_{\Gamma}(\mathcal{T}_n)}\int_e\mathbf{n}\cdot(\mathcal{A}\nabla_n\overline{(z-z_n)})u_n\,ds\\
&+\sum_{e\in\mathcal{E}_{\Gamma}(\mathcal{T}_n)}\int_e\mathsf{c}\,u_n\overline{(z-z_n)}\,ds\ ,\end{aligned}$$

which is equivalent to $\sum_{K\in\mathcal{T}_n}\eta_K$. □

Since we are interested in the accurate computation of the modes supported by the metallic waveguide, we introduce the following definition for the functional of interest

$$J(\hat{v}):=\delta\|v\|^2_{0,\mathcal{C}}\ , \tag{17}$$

where $\hat{v}:=(\delta,v)$, in such case we have

$$J(\hat{u})-J(\hat{u}_n)=\lambda-\lambda_n\ ,$$

because we have assumed that all eigenfunction are normalized, i.e. $\|u\|_{0,\mathcal{C}}=\|u_n\|_{0,\mathcal{C}}=1$. Then we use the definition of $J(\cdot)$ from (17) to write down explicitly the Fréchet derivative of $J(\cdot)$ and of $\mathcal{N}(\cdot,\cdot)$ at $\hat{u}$:

$$J'[\hat{u}](\hat{v}):=\lambda b(u,v)+\lambda b(v,u)+\delta\|u\|^2_{0,\mathcal{C}}\ ,$$

and

$$\mathcal{N}'[\hat{u}](\hat{v},\hat{z}) := -A_n(v,z) + \lambda b(v,z) + \delta b(u,z) + \beta b(u,v) + \beta b(v,u) \ ,$$

with $\hat{v} := (\delta, v)$ and $\hat{z} := (\beta, z)$. Since $\hat{u}$ is unavailable, we introduce an auxiliary problem — which is an approximation of problem (13) — which is based on the computable approximation $\hat{u}_n$:

$$\mathcal{N}'[\hat{u}_n](\hat{v},\hat{z}) = J'[\hat{u}_n](\hat{v}) \ . \tag{18}$$

This leads to the following linear problem, which has a unique solution: *seek* $\hat{z} := (\beta, z) \in \mathbb{C} \times S$*, such that*

$$-A_n(v,z)+\lambda_n b(v,z)+\delta b(u_n,z)+\beta b(u_n,v)+\beta b(v,u_n) = \lambda_n b(u_n,v)+\lambda_n b(v,u_n)+\delta\|u_n\|^2_{0,\mathcal{C}} \ ,$$

for all $(\delta, v) \in \mathbb{C} \times S$.

It should be clear from the definition of η_K in Theorem 4.2 that these quantities are not explicitly computable, in general. In order to obtain a computable quantity, the dual solution $\hat{z}$ must be approximated in some suitable finite element space. Apparently the approximation $z_n \in S_n$ is of no use, because $\mathcal{N}(\hat{u}_n, \hat{z}_n - \hat{z}_n) = 0$. In practice, it is necessary to compute an approximation of z in a space $\tilde{S}_n$ which is "richer" than S_n. Probably the simpler choice to construct a richer space is to maintain the same partition, but increase the local polynomial degree by one on each element.

5. Adaptive Algorithms

The *hp*-adaptive algorithm used for the numerical experiments in Section 6 is detailed below in Algorithm 1.

Algorithm 1 Goal-oriented adaptive algorithm

$(\lambda_{j,n}, u_{j,n}, \mathcal{T}_{j,n}, S_n) := \text{GoalDG}(\mathcal{T}_0, S_0, j, \theta, \text{tol}, J(\cdot))$
$n = 0$
repeat
  Compute the j-th eigenpair $(\lambda_{j,n}, u_{j,n})$ on $\mathcal{T}_n$
  $\tilde{S}_n := \text{DualSpace}(\mathcal{T}_n, S_n)$
  Compute $(\tilde{\beta}_n, \tilde{z}_n) \in \mathbb{C} \times \tilde{S}_n$ solving the linear problem (18) on $\mathcal{T}_n$
  Compute η_K for all $K \in \mathcal{T}_n$
  if $\left|\sum_{K\in\mathcal{T}_n} \eta_K\right| < \text{tol}$ **then**
    exit
  else
    $(\mathcal{T}_{n+1}, S_{n+1}) := \text{Refine}(\mathcal{T}_n, S_n, \theta, \{\eta_K\}_{K\in\mathcal{T}_n})$
    $n = n + 1$
  end if
until

The algorithm takes as input: an initial mesh $\mathcal{T}_0$, an initial DG space S_0, the index j of the eigenpair to approximate, a real value $0 \leq \theta \leq 1$ to tune the marking strategy, a real and positive value tol which prescribes the required tolerance, and finally the goal functional $J(\cdot)$ that should be used. The algorithm has a very simple structure that consists of a repeat-until loop. During each iteration of the loop a new approximation of the eigenpair of interest is computed, then the finer space $\tilde{S}_n$ is constructed and an approximate solution $(\tilde{\delta}_n, \tilde{z}_n)$ of problem (18) is computed. Finally the error estimator is calculated and, if the estimated error $\left|\sum_{K\in\mathcal{T}_n} \eta_K\right|$ is lower than the prescribed tolerance tol the algorithm stops; otherwise the mesh $\mathcal{T}_n$ and the space S_n are refined and another iteration follows. To complete the description of the algorithms we must describe the function DualSpace and Refine.

The function Refine applies a simple fixed-fraction strategy to mark a minimal subset of elements containing a portion of the error proportional to θ. Then the choice for each marked element between splitting the element into smaller elements (h-refinement) or increasing the polynomial order (p-refinement) is made by testing the local analyticity of the solution in the interior of the element as described in [17]. The function DualSpace constructs the space $\tilde{S}_n$ by increasing by 1 the order of polynomials in each element in S_n.

6. Numerical experiments

In this section we have collected numerical results using our a posteriori error estimator with the clear aim to show the robustness of the error estimator and the fast decay of the error on a sequence of *hp*-adapted meshes. Since we are most interested in testing the adaptive method in the possible most difficult case, we set up a problem with $\mathcal{A}$ equal to 1.52 in Ω_{out} and equal to $-11.8 + 1.23i$ in Ω_{in}, also we choose $\mathcal{B} = 0$ and $\mathcal{C} = 1$. The values of $\mathcal{A}$ are chosen to represent real materials. The reason why we only choose to play with the values of $\mathcal{A}$ is because a jump in the coefficient of the second order term of the operator can lead to strong singularities in the gradient of the eigenfunctions. These local singularities are hard to resolve with standard finite element methods and pose a challenging test for our method. Discontinuities in $\mathcal{B}$ or $\mathcal{C}$ do not pose the same kind of difficulties.

Following [18], we assume an error model of the form

$$\lambda_n = \lambda + Ce^{-2a\sqrt[3]{\text{DOFs}}},$$

for problems with discontinuous coefficients, whose eigenfunctions are expected to have isolated singularities. The constants C and a are determined by least-squares fitting, and a is reported for each problem.

Plots are given of the relative error for eigenvalues $|\lambda - \lambda_n|/|\lambda_n|$, the correspondent relative value of the a posteriori error estimator $|\eta|/|\lambda_n|$ and the associated effectivity index, which is defined as $|\lambda - \lambda_n|/\eta$. In order to visually appreciate the converge rate of the *hp*-adaptive method, we plot a red line computed with the least-squares fitting method to highlight the slope of the curve.

As reference solutions for problems in this section we use highly accurate computations on very rich finite element spaces to produce "exact eigenvalues" for our comparisons.

All the experiments have been carried out using AptoFEM (`www.aptofem.com`) on a single processor desktop machine. In particular, we used ARPACK [19] to compute the eigenvalues and MUMPS [20] to solve the linear systems.

The eigenpair that we have decide to compute is one of those vanishing modes concentrated on the surface of the metallic fibre and it has multiplicity 2. In Figure 1a we have reported the initial mesh and the distribution of different materials in the domain. The red part correspond to the metallic waveguide. Figure 2a shows the convergence of the relative error for eigenvalues and the decay of the relative error estimator as well. As can be seen

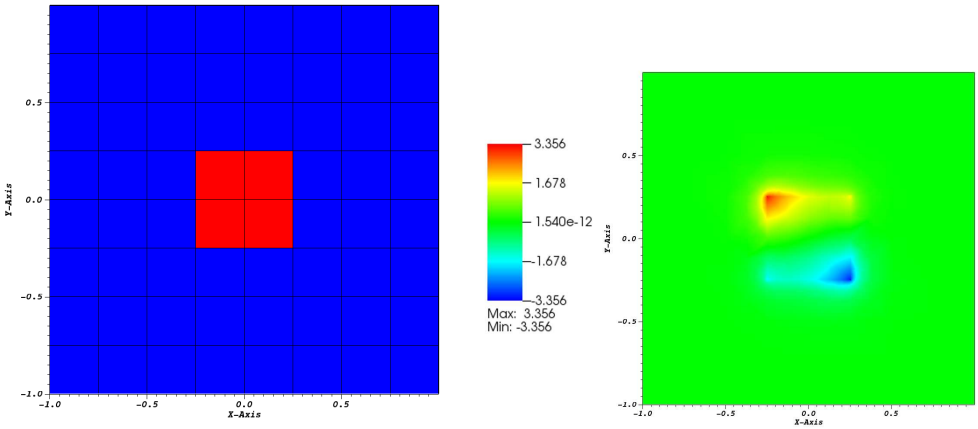

(a) (b)

Figure 1: (a) Distribution of different materials in the domain and initial mesh. In red we have the section of the metallic waveguide. (b) Real part of the eigenfunction.

the two curves are very close together remarking the reliability and accuracy of this error estimator. This is very different from the performance of the explicit error estimator presented in [4] for similar problems. Clearly the extra computational work necessary to compute the solution of the dual problem leads to much more accurate estimations of the error. This is further supported by the values of the efficiency index reported in Figure 2b which are close to 1.

In Figure 1b we reported the real part of the eigenfunction of interest. As can be seen the mode is well concentrated on the border of the metallic fibre and it presents local singularity in the gradient at the corners of the waveguide. Especially on two corners the singularities seem stronger.

In Figure 3a we reported the real part of the eigenfunction of interest with the adapted mesh after 9 iterations of the adaptive algorithm. The fact that the refinement concentrate mostly around two of the corners suggests that stronger singularities are present there. Finally in Figure 3b we have the adapted mesh and order of polynomials after 9 iterations of the adaptive algorithm. High order elements in the interior of the waveguide are indication that the eigenfunction is smooth inside the waveguide.

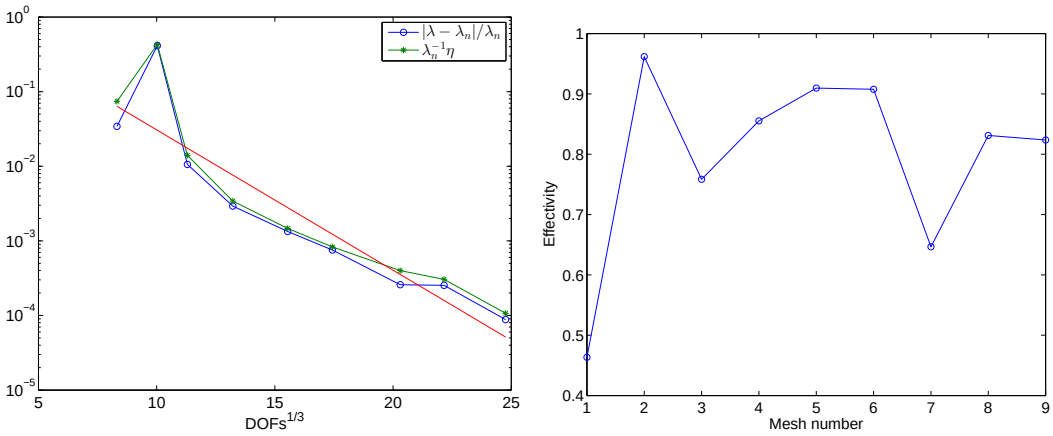

(a) (b)

Figure 2: (a) Plot of the relative error for eigenvalues and relative value of the error estimator. The red line represent the estimated convergence rate of $a = 0.2165$. (b) Efficiency index for the $hp-$adaptive method.

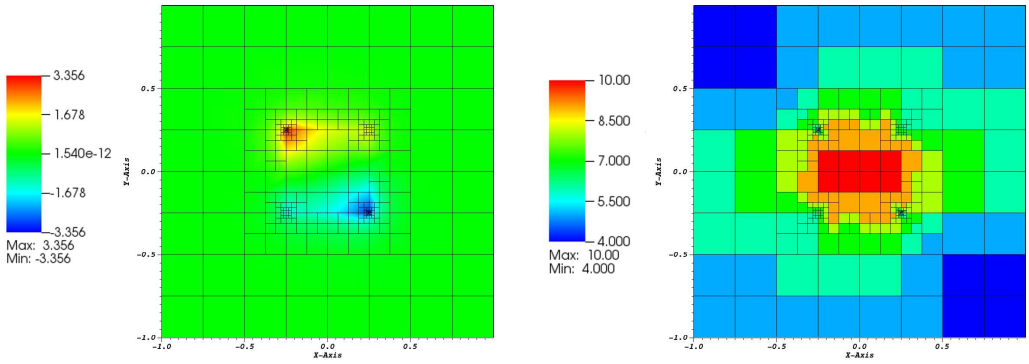

(a) (b)

Figure 3: (a) Refined mesh after 9 iterations and real part of the eigenfunction. (b) Adapted mesh after 9 iterations. The color scheme indicates different order of polynomials used in the elements.

References

[1] S. Giani, L. Grubišić, J. S. Ovall, Benchmark results for testing adaptive finite element eigenvalue procedures, Appl. Numer. Math. 62 (2) (2012) 121–140.

[2] P. Berini, Plasmon-polariton waves guided by thin lossy metal films of finite width: Bound modes of symmetric structures, Physical Review B 61 (15) (2000) 10484+.

[3] M. Marletta, Eigenvalue problems on exterior domains and Dirichlet to Neumann maps, J. Comput. Appl. Math. 171 (1-2) (2004) 367391.

[4] S. Giani, An a posteriori error estimator for hp-adaptive continuous galerkin methods for photonic crystal applications, Computing 95 (5) (2013) 395–414.

[5] D. N. Arnold, F. Brezzi, B. Cockburn, L. D. Marini, Unified analysis of discontinuous Galerkin methods for elliptic problems, SIAM J. Numer. Anal. 39 (5) (2001) 1749–1779.

[6] A. Ern, A. F. Stephansen, P. Zunino, A discontinuous Galerkin method with weighted averages for advectiondiffusion equations with locally small and anisotropic diffusivity, IMA J. Numer. Anal. 29 (2) (2009) 235 –256.

[7] R. Hartmann, P. Houston, Error estimation and adaptive mesh refinement for aerodynamic flows, in: H. Deconinck (Ed.), VKI LS 2010-01: 36^{th} CFD/ADIGMA course on hp-adaptive and hp-multigrid methods, Oct. 26-30, 2009, Von Karman Institute for Fluid Dynamics, Rhode Saint Genèse, Belgium, 2009.

[8] P. Houston, C. Schwab, E. Süli, Discontinuous hp-finite element methods for advection-diffusion-reaction problems, SIAM J. Numer. Anal. 39 (6) (2002) 2133–2163.

[9] P. Houston, D. Schötzau, T. Wihler, Energy norm a posteriori error estimation of *hp*–adaptive discontinuous Galerkin methods for elliptic problems, Math. Mod. Meth. Appl. Sci. 17 (1) (2007) 33–62.

[10] T. Leicht, R. Hartmann, Error estimation and *hp*–adaptive mesh refinement for discontinuous Galerkin methods, in: Z. J. Wang (Ed.), Adaptive High-Order Methods in Computational Fluid Dynamics, Vol. 2, chapter 3 of Advances in Computational Fluid Dynamics, World Science Books, 2011, pp. 67–94.

[11] L. Zhu, S. Giani, P. Houston, D. Schötzau, Energy norm a-posteriori error estimation for hp-adaptive discontinuous Galerkin methods for elliptic problems in three dimensions, Math. Mod. and Meth. in App. Sci. (M3AS) 21 (2) (2011) 267–306.

[12] S. Giani, E. Hall, An a posteriori error estimator for hp-adaptive discontinuous Galerkin methods for elliptic eigenvalue problems, Math. Mod. and Meth. in App. Sci. (M3AS), submitted.

[13] L. Zhu, S. Giani, P. Houston, D. Schötzau, Energy norm a-posteriori error estimation for *hp*-adaptive discontinuous Galerkin methods for eliptic problems in three dimensions, Math. Mod. and Meth. in App. Sci. (M3AS) 21 (2) (2011) 267–306.

[14] M. Petzoldt, A posteriori error estimators for elliptic equations with discontinuous coefficients, Adv. Comput. Math. 16 (1) (2002) 47–75.

[15] R. Becker, R. Rannacher, An optimal control approach to a posteriori error estimation in finite element methods, Acta Numer. 10 (2001) 1–102.

[16] V. Heuveline, R. Rannacher, A posteriori error control for finite approximations of elliptic eigenvalue problems, Adv. Comput. Math. 15 (1-4) (2001) 107–138.

[17] P. Houston, E. Süli, A note on the design of *hp*-adaptive finite element methods for elliptic partial differential equations, Comput. Methods Appl. Mech. Engrg. 194 (2-5) (2005) 229–243.

[18] I. Babuška, B. Q. Guo, The h-p version of the finite element method for domains with curved boundaries, SIAM J. Numer. Anal. 25 (4) (1988) 837–861.

[19] R. B. Lehoucq, D. C. Sorensen, C. Yang, ARPACK Users' Guide: Solution of Large Scale Eigenvalue Problems with Implicitly Restarted Arnoldi Methods, SIAM, 1998.

[20] P. Amestoy, I. Duff, J.-Y. L'Excellent, Multifrontal parallel distributed symmetric and unsymmetric solvers, Comput. Methods in Appl. Mech. Eng. 184 (2–4) (2000) 501–520.